Method for eliminating mismatching error in monolithic triaxial ring resonators

Xingwu Long (龙兴武) and Jie Yuan (袁　杰)*

Department of Optoelectronic Engineering, College of Optoelectronic Science and Engineering, National University of Defense Technology, Changsha 410073, China

**E-mail: jieyuan@nudt.edu.cn*

Received April 22, 2010

Several results on optical-axis perturbation and elimination of the mismatching error C of a monolithic triaxial ring resonator (MTRR) are reported. Based on the augmented 5×5 ray matrix method, by simultaneously considering axial displacement of a mirror and the misalignments in three planar square ring resonators of a MTRR, the rules of optical-axis perturbation are obtained. The mismatching error C of the MTRR is eliminated. The results obtained are important for cavity design, as well as in the improvement and alignment of MTRR.

OCIS codes: 140.4780, 140.3410, 140.3370, 140.3560.

doi: 10.3788/COL20100812.1135.

This letter is a continuation of Ref. [1]. Ring laser has been used as a rotate sensor. The planar or non-planar resonator, as well as monoaxial or monolithic triaxial ring resonator (MTRR), have been widely used for laser gyroscopes[2−9]. Continuous research on optical-axis perturbation in ring resonators have been conducted[10−15]. However, the perturbation sources in all the previous articles have been on radial displacements or angular misalignments of the optical components of the ring resonator. The perturbation source of the axial displacement of a mirror has not been previously discussed. The augmented 5×5 ray matrix method is used to handle these perturbation sources.

The ray matrix of a general optical component with angular misalignment and radial displacements has the form:

$$\begin{pmatrix} r_{\mathrm{ox}} \\ r'_{\mathrm{ox}} \\ r_{\mathrm{oy}} \\ r'_{\mathrm{oy}} \\ 1 \end{pmatrix} = \begin{pmatrix} A_x & B_x & 0 & 0 & E_x \\ C_x & D_x & 0 & 0 & F_x \\ 0 & 0 & A_y & B_y & E_y \\ 0 & 0 & C_y & D_y & F_y \\ 0 & 0 & 0 & 0 & 1 \end{pmatrix} \begin{pmatrix} r_{\mathrm{ix}} \\ r'_{\mathrm{ix}} \\ r_{\mathrm{iy}} \\ r'_{\mathrm{iy}} \\ 1 \end{pmatrix}, \quad (1)$$

where r_{ix}, r_{iy}, r_{ox}, and r_{oy} are the input ray and output ray heights from the reference axis along the x and y axes; this is referred to as optical-axis decentration. Then, r'_{ix}, r'_{iy}, r'_{ox}, and r'_{oy} are the angles that the input and output rays construct with the reference axis in the x and y planes, respectively; this is referred to as optical-axis tilts. In Fig. 1, x axis has been chosen as an example to show the parameters. A_x, B_x, C_x, and D_x are the standard ray-matrix elements in the tangential plane; A_y, B_y, C_y, and D_y are the standard ray-matrix elements in the sagittal plane; and E_x and E_y are the decentration terms representing radial displacements along x and y axes. F_x and F_y are the tilt terms representing the angular misalignments. In the case of a mirror, $F_x = 2\tan(\theta_x)$, $F_y = 2\tan(\theta_y)$, and θ_x and θ_y are the misalignment angles in its local tangential and sagittal planes, respectively.

In Fig. 2[1], a spherical mirror has been chosen as an example to show the perturbation sources. M and M' represent the mirrors before and after axial displacement δ along the normal z direction. Axes x and y are perpendicular to z. Generally, the mirror has six movements, which are the displacements along the x, y, and z axes, and the rotations around the x, y, and z axes. The translation of the mirror along the x and y axes manifests as radial displacements represented by E_x and E_y in the augmented 5×5 matrix.

The rotary movements around the axes of x and y are the angular misalignments of the mirror, and they can be represented by the terms F_y and F_x in the augmented 5×5 matrix. The rotation of the mirror around the axis z can be ignored because it has spherical symmetry. In this letter, the displacement of the mirror along the z axis is called axial displacement. It cannot be represented by any term in the augmented 5×5 matrix in the current framework of the study. Thus far, this axial displacement has not been discussed in detail.

In this letter, the axial displacement of the mirror is treated as the source of perturbation along with the misalignments. The augmented 5×5 ray matrix is modified to include this perturbation. To the best of our knowledge, this is the first time that such axial displacement has been considered as a perturbation source. The square ring resonator and MTRR are chosen as examples to show its application. Optical-axis perturbation induced by the axial displacement of the spherical mirror and the corresponding misalignments can be obtained by utilizing the modified 5×5 ray matrix. The method for reducing,

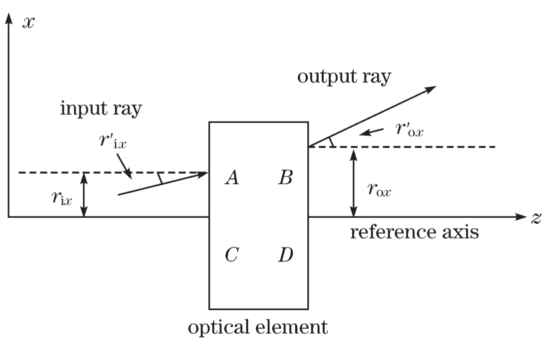

Fig. 1. Schematic diagram of the input and output rays.

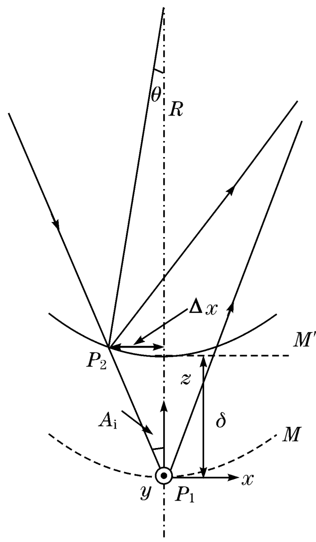

Fig. 2. Schematic diagram of mirror displacement.

and even eliminating, the mismatching error in MTRR has been determined; this is the purpose of the present work.

As shown in Fig. 2[1], the axial displacement of the mirror influences ray transfer. When the spherical mirror has a small axial displacement δ along the z axis, the reflection point changes from P_1 to P_2. For a linear resonator, the ray is a vertical incidence and A_i=0. The distance between P_1 and P_2 becomes 0 and the reflection point does not change under the axial displacement δ condition. For a ring resonator, the ray is not a vertical incidence and $A_\mathrm{i} \neq 0$. The distance between P_1 and P_2 is

$$\Delta x = \delta \cdot \tan(A_\mathrm{i}). \tag{2}$$

An angle of θ is generated between the two normal directions before and after axial displacement. This is represented by

$$\theta = \frac{\Delta x}{R} = \frac{\delta \tan(A_\mathrm{i})}{R}, \tag{3}$$

where R is the radius of the curvature equivalent to an angular misalignment of θ along the y axis represented by F_x. The augmented 5×5 ray matrix of a reflective spherical mirror M_i with axial displacement can be expressed as

$$M(M_i) = \begin{bmatrix} 1 & 0 & 0 & 0 & 0 \\ -\frac{2}{R_i \times \cos A_\mathrm{i}} & 1 & 0 & 0 & 2[\theta_{ix} + \delta_i \cdot \tan(A_\mathrm{i})/R_i] \\ 0 & 0 & 1 & 0 & 0 \\ 0 & 0 & -\frac{2 \times \cos A_\mathrm{i}}{R_i} & 1 & 2\theta_{iy} \\ 0 & 0 & 0 & 0 & 1 \end{bmatrix}. \tag{4}$$

The effect of axial displacement on optical-axis perturbation can be obtained by solving the eigenvector of the total round-trip matrix of the ring resonator. The misalignment-induced optical-axis perturbations of the mirror in square ring resonator and the triaxial ring resonator have been discussed in our previous works[1,14,15]. A square ring resonator has been chosen as an example. As shown in Fig. 3[1], $\delta_i (i = a, b)$ represents the axial displacement of mirror M_i (i=a,b).

All three planar ring resonators are square ring resonators; they are mutually orthogonal. A square ring resonator is shown in Fig. 3[1]. Mirrors M_a and M_b are spherical mirrors, while mirrors M_c and M_d are flat mirrors. The incident angle is 45°. Points P_a, P_b, P_c, and P_d are the terminal points of the resonator. The diaphragm is located at point P_e, the midpoint between the two spherical mirrors, P_a and P_b. The optical-axis perturbation at point P_e caused by the misalignments and axial displacements of the spherical mirror can be written as

$$\Delta x_e = \frac{\sqrt{2}}{4}[R(\theta_{ax} + \theta_{bx}) + \delta_a + \delta_b],$$

$$\Delta y_e = \frac{\sqrt{2}}{2} R(\theta_{ay} + \theta_{by}). \tag{5}$$

The optical-axis locations x_e and y_e are the optical-axis deviations from the longitudinal axis of the ideal diaphragm along the x and y axes, respectively. Δx_e and Δy_e are the optical-axis perturbations in x and y axes, respectively. As shown in Fig. 3[1], the positive orientation of y_e is upward and perpendicular to the plane of the resonator. The positive orientation of x_e is shown as the black arrow located at point P_e. The positive orientation of δ_a is shown as the black arrow pointing to the center of the resonator. The positive orientation of δ_b is shown as the black arrow pointing to the center of the resonator. The misalignment angles, θ_{ax}, θ_{ay}, θ_{bx}, and θ_{by}, have been defined in Ref. [1].

As shown in Fig. 4[1], M_1, M_2, M_3, M_4, M_5, and M_6 are positioned in the center of each body face of a cube. The cube was crafted such that a small diameter bore connects adjacent mirrors. A closed optical cavity was set between four coplanar mirrors interconnected by bores. There were three mutually orthogonal closed beam paths, each of which was used to detect angular rotation around its normal axis. The planar ring resonator, defined by the optical cavity between M_2, M_3, M_4, and M_6, is called cav-

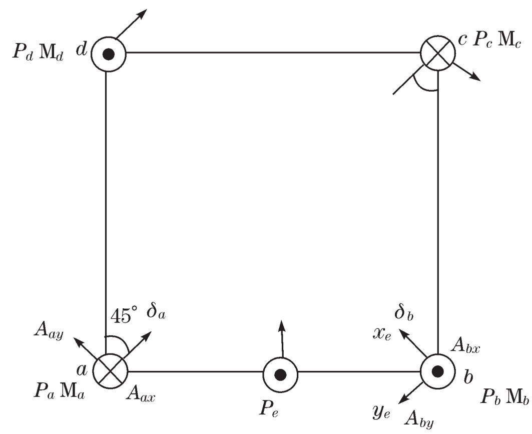

Fig. 3. Schematic diagram of a square ring resonator.

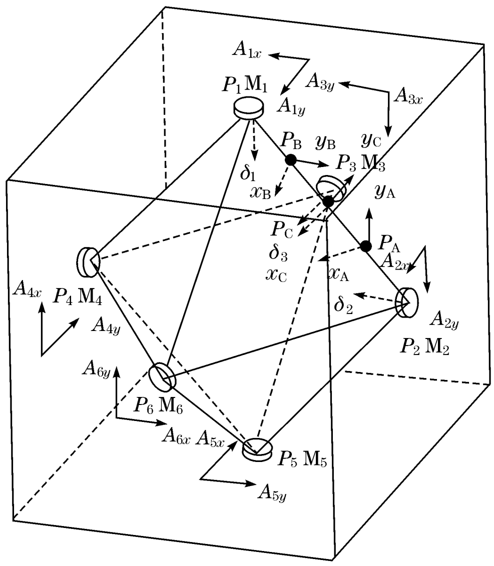

Fig. 4. Schematic diagram of monolithic triaxial ring resonator with spherical mirror's axial displacement.

ity A; the resonator, defined by M_1, M_3, M_5, and M_6, is called cavity B; and the resonator, defined by M_1, M_2, M_5, and M_4, is called cavity C. M_1, M_2, and M_3 are spherical mirrors with common radius R, while M_4, M_5, and M_6 are flat mirrors. Points P_1, P_2, P_3, P_4, P_5, and P_6 were set as the terminal points of the resonator.

P_A, P_B, and P_C, the diaphragms of the cavities A, B, and C, respectively, were chosen for analysis. For MTRR, the optical-axes of all three monoaxial ring resonators passed through the center of their diaphragms simultaneously. As shown in Fig. 4[1], the positive orientations of x_A, y_A, x_B, y_B, x_C, and y_C, as well as the misalignment angles of θ_{ix} and θ_{iy} (i=1,2,3,4,5,6), are set based on what is indicated in Ref. [1]. As shown in Fig. 4, δ_1, δ_2, and δ_3 are the axial displacements of M_1, M_2, and M_3, respectively. The optical-axis perturbations at P_A, P_B, and P_C caused by the misalignments and axial displacements of the spherical mirror can be written as

$$\begin{array}{l} \Delta x_A = \frac{\sqrt{2}}{4}[R(\theta_{2y}-\theta_{3x})+\delta_2+\delta_3] \\ \Delta y_A = \frac{\sqrt{2}}{2}R(\theta_{2x}-\theta_{3y}) \end{array}, \tag{6}$$

$$\begin{array}{l} \Delta x_B = \frac{\sqrt{2}}{4}[R(\theta_{3y}-\theta_{1x})+\delta_1+\delta_3] \\ \Delta y_B = \frac{\sqrt{2}}{2}R(\theta_{3x}-\theta_{1y}) \end{array}, \tag{7}$$

and

$$\begin{array}{l} \Delta x_C = \frac{\sqrt{2}}{4}[R(\theta_{1y}-\theta_{2x})+\delta_1+\delta_2] \\ \Delta y_C = \frac{\sqrt{2}}{2}R(\theta_{1x}-\theta_{2y}) \end{array}. \tag{8}$$

Equations (6)−(8) can be modified as

$$\begin{array}{l} R(\theta_{2y}-\theta_{3x})+\delta_2+\delta_3 = 2\sqrt{2}\times\Delta x_A \\ R(\theta_{2x}-\theta_{3y}) = \sqrt{2}\times\Delta y_A, \end{array}, \tag{9}$$

$$\begin{array}{l} R(\theta_{3y}-\theta_{1x})+\delta_1+\delta_3 = 2\sqrt{2}\times\Delta x_B \\ R(\theta_{3x}-\theta_{1y}) = \sqrt{2}\times\Delta y_B \end{array}, \tag{10}$$

and

$$\begin{array}{l} R(\theta_{1y}-\theta_{2x})+\delta_1+\delta_2 = 2\sqrt{2}\times\Delta x_C \\ R(\theta_{1x}-\theta_{2y}) = \sqrt{2}\times\Delta y_C \end{array}. \tag{11}$$

We could then obtain the following equations:

$$\begin{aligned} &[R(\theta_{2y}-\theta_{3x}+\theta_{2x}-\theta_{3y}+\theta_{3y}-\theta_{1x}+\theta_{3x}-\theta_{1y} \\ &+\theta_{1y}-\theta_{2x}+\theta_{1x}-\theta_{2y})]+(2\delta_1+2\delta_2+2\delta_3) \\ &=2\sqrt{2}\times\Delta x_A+\sqrt{2}\times\Delta y_A+2\sqrt{2}\times\Delta x_B \\ &+\sqrt{2}\times\Delta y_B+2\sqrt{2}\times\Delta x_C+\sqrt{2}\times\Delta y_C, \end{aligned} \tag{12}$$

$$\begin{aligned} &\Delta x_A+\Delta y_A/2+\Delta x_B+\Delta y_B/2+\Delta x_C+\Delta y_C/2 \\ &=\frac{\sqrt{2}}{2}(\delta_1+\delta_2+\delta_3). \end{aligned} \tag{13}$$

The equations are different from the optical-axis perturbation caused by the misalignment of the mirror, which was 0 in Ref. [1]. Thus, we used the functions $x_A(t)$, $y_A(t)$, $x_B(t)$, $y_B(t)$, $x_C(t)$, and $y_C(t)$ to represent the optical-axis locations at time of t. When $t = 0$, the optical-axis locations at P_A, P_B, and P_C can be written as $x_A(0)$, $y_A(0)$, $x_B(0)$, $y_B(0)$, $x_C(0)$, and $y_C(0)$. The optical-axis perturbations for the period 0 to t can be written as

$$\begin{aligned} \Delta x_A(0\to t) &= x_A(t)-x_A(0), \\ \Delta y_A(0\to t) &= y_A(t)-y_A(0), \\ \Delta x_B(0\to t) &= x_B(t)-x_B(0), \\ \Delta y_B(0\to t) &= y_B(t)-y_B(0), \\ \Delta x_C(0\to t) &= x_C(t)-x_C(0), \\ \Delta y_C(0\to t) &= y_C(t)-y_C(0). \end{aligned} \tag{14}$$

According to Eq. (13),

$$\begin{aligned} &\Delta x_A(0\to t)+\Delta y_A(0\to t)/2+\Delta x_B(0\to t) \\ &+\Delta y_B(0\to t)/2+\Delta x_C(0\to t)+\Delta y_C(0\to t)/2 \\ &=\frac{\sqrt{2}}{2}(\delta_1+\delta_2+\delta_3). \end{aligned} \tag{15}$$

From Eqs. (14) and (15), we can obtain[1]

$$\begin{aligned} &x_A(t)+y_A(t)/2+x_B(t)+y_B(t)/2+x_C(t)+y_C(t)/2 \\ &=x_A(0)+y_A(0)/2+x_B(0)+y_B(0)/2+x_C(0) \\ &+y_C(0)/2+\frac{\sqrt{2}}{2}(\delta_1+\delta_2+\delta_3) \\ &=C. \end{aligned} \tag{16}$$

The distances between the optical axis and the center of the diaphragm at any point of P_A, P_B, and P_C can be written as D_A, D_B, and D_C[1]:

$$\begin{aligned} D_A &= \sqrt{x_A^2+y_A^2}, \\ D_B &= \sqrt{x_B^2+y_B^2}, \\ D_C &= \sqrt{x_C^2+y_C^2}. \end{aligned} \tag{17}$$

The three monoaxial ring resonators cannot be simultaneously aligned to the best condition of $D_A = D_B = D_C = 0$ when $C \neq 0$. To obtain the lowest value of the total diffraction loss of the monolithic triaxial ring resonator, the smallest values of D_A, D_B, and D_C should be employed simultaneously; that is, the mismatching error should be shared equally[1]. Therefore, the best case should be

$$\begin{aligned} &x_A(t) = x_B(t) = x_C(t) = C/3, \\ &y_A(t) = y_B(t) = y_C(t) = 0, \\ &D_A = D_B = D_C = \frac{|C|}{3}. \end{aligned} \tag{18}$$

Equation (16), the result from Ref. [1], is no longer valid. The mismatching error C of the MTRR is not invariant; that is, it can be variable because of the influence of the axial displacement of the spherical mirror. Whether the mismatch error C of the MTRR at the time of $t = 0$ is big or small, the mismatching error at the time of t can be decreased, and even eliminated, by choosing the appropriate δ_1, δ_2, and δ_3. If δ_1, δ_2, and δ_3 satisfy the following condition:

$$\begin{aligned} \delta_1 + \delta_2 + \delta_3 = -\sqrt{2} \times [&x_A(0) + y_A(0)/2 \\ &+ x_B(0) + y_B(0)/2 + x_C(0) + y_C(0)/2], \end{aligned} \tag{19}$$

then

$$\begin{aligned} &x_A(t) + y_A(t)/2 + x_B(t) + y_B(t)/2 \\ &+ x_C(t) + y_C(t)/2 = 0. \end{aligned} \tag{20}$$

Consequently, the following ideal condition can be obtained:

$$\begin{aligned} &x_A(t) = x_B(t) = x_C(t) = 0, \\ &y_A(t) = y_B(t) = y_C(t) = 0, \\ &D_A = D_B = D_C = 0. \end{aligned} \tag{21}$$

D_A, D_B, and D_C, the distances between the optical axis and the center of the diaphragm at any point of P_A, P_B, and P_C, were simultaneously reduced to their smallest values. Additionally, the total diffraction loss of the monolithic triaxial ring resonator was at its lowest.

In conclusion, we investigate the axial displacement-induced optical-axis perturbation of a mirror by modifying the augmented 5×5 matrix in consideration of its axial displacement. The mismatching error C of the triaxial ring resonator cannot be decreased by modifying the angles of the terminal surfaces or the terminal mirrors[1]. When $C \neq 0$, the three monoaxial ring resonators cannot be simultaneously aligned to the best condition. An optimization method that can share the mismatching error C is proposed in Ref. [1]. The method entails equal and simultaneous sharing of mismatching error C among three specific directions, x_A, x_B, and x_C. By simultaneously considering the axial displacement and misalignments of the mirror, the mismatching error C of the MTRR can be eliminated by choosing the appropriate axial displacements of the spherical mirrors. D_A, D_B, and D_C can then be reduced to their smallest values, and the total diffraction loss of the monolithic triaxial ring resonator can be at its lowest. The optical-axes of all three monoaxial ring resonators in MTRR can be made to pass through the center of their diaphragms simultaneously by properly controlling the perturbation source of axial displacement. By utilizing this method, the alignment precision can be greatly improved and the total diffraction loss can be reduced in MTRR.

This work was supported by the National Natural Science Foundation of China under Grant Nos. 60608002 and 60608002.

References

1. J. Yuan, X. W. Long, and L. M. Liang, Appl. Opt. **47,** 628 (2008).
2. W. W. Chow, J. Gea-Banacloche, L. M. Pedrotti, V. E. Sanders, W. Schleich, and M. O. Scully, Rev. Mod. Phys. **57,** 61 (1985).
3. M. Faucheux, D. Fayoux, and J. J. Roland, J. Optics (Paris) **19,** 101 (1988).
4. J. C. Stiles and B. H. G. Ljung, "Monolithic three axis ring laser gyroscope" US Patent 4,477,188 (Oct. 16, 1984).
5. A. E. Siegman, IEEE J. Sel. Top. Quantum Electron. **6,** 1389 (2000).
6. Z. Wang, X. Long, F. Wang, Z. Tan, and F. Xu, Acta Opt. Sin. (in Chinese) **28,** 301 (2008).
7. Z. Wang, X. Long, and F. Wang, Acta Opt. Sin. (in Chinese) **29,** 2892 (2009).
8. Z. Wang, X. Long, F. Wang, and J. Yuan, Acta Opt. Sin. (in Chinese) **29,** 3202 (2009).
9. Z. Wang, X. Long, F. Wang, and Y. Huang, Chinese J. Lasers (in Chinese) **37,** 713 (2010).
10. I. W. Smith, Proc. SPIE **412,** 203 (1983).
11. A. H. Paxton and W. P. Latham, Jr., Appl. Opt. **25,** 2939 (1986).
12. R. Rodloff, IEEE J. Quantum Electron. **23,** 438 (1987).
13. S.-C. Sheng, Opt. Lett. **19,** 683 (1994).
14. J. Yuan, X. W. Long, B. Zhang, F. Wang, and H. C. Zhao, Appl. Opt. **46,** 6314 (2007).
15. J. Yuan and X. W. Long, Opt. Commun. **281,** 1204 (2008).